Proceedings of The Institute of Acoustics

Glint and its effect on the Accuracy of a Sea Bed Profiling Sonar

P.N.Denbigh

Department of Electronic and Electrical Engineering,
University of Birmingham, Birmingham B15 2TT

Introduction

The term 'glint' is used in radar and refers to the displacement between the measured direction of a target and its true direction (1)(2). It exists because the wavefront of the echo is slightly crinkled such that a measurement of the wavefront angle at a particular point in space indicates that the wave has emanated from somewhere other than its true origin. The same phenomenon is relevant in a new type of sea bed profiling sonar known as a 'bathymetric side-scan sonar'(3).

As with a conventional sidescan sonar the bathymetric sidescan sonar transmits short pulses of sound confined to a vertical fan beam pointing broadside to the direction of the ships motion. The bathymetric sidescan sonar however has a different receive system compared with the conventional sidescan sonar and it is this difference which enables it to rapidly produce profiles of the insonified swath as well as the usual measurements of backscattered amplitude. The bathymetric sidescan has two receivers one above the other which are quite separate from the transmitter. Short tone bursts are transmitted and the phase difference between the two backscattered receive signals is measured. From this measurement the angle of the incident wavefront may be deduced and hence the declination angle θ of the region of the sea bed from which the wavefront originated can be obtained. This declination angle is measured continuously as the transmitted pulse propagates outwards striking successive regions of the insonified swath in turn. The range R is available from the two-way propagation time and the depth of each point along the swath may therefore be obtained from $R \sin \theta$. Plotted against the horizontal range $R \cos \theta$ a true sea bed profile is obtained but in many cases a plot of depth versus slant range R is an adequate approximation. The profiles are displayed on a fibre optic recorder, one for each transmitted pulse. At the high pulse repetition frequencies used an excessive number of profiles usually ensues and alternative techniques for displaying the depth information are generally preferred. These include depth-modulated sidescan displays and stereoscopic amplitude-modulated sidescan displays (3)(4). The accuracy of depth measurement depends on many factors amongst which multipath interference and transducer dissimilarity are the most important. However multipath interference can be largely eliminated by side-baffles (5) and transducer dissimilarity can be avoided by careful design and construction. The major remaining limitation to accuracy is the glint phenomenon.

The Glint Phenomenon in Sea Bed Profiling

The geometry of a conventional sidescan sonar is shown in Fig.1, and Fig.2 demonstrates the principle of the bathymetric sidescan sonar by showing small sections of the backscattered wavefronts 'frozen' at a particular instant in time. The wavefronts shown originate from different regions of the sea bed. The fundamental assumption of the depth measuring technique is that a particular wavefront is circular in the vertical plane and is centred about the small region of the sea bed from which it has originated. In this way a measurement of the angle of the incident wavefront, obtained by measuring the phase difference between two transducers, can give the declination angle of that sea bed region.

Fig.2 is useful in explaining the principle of the bathymetric sidescan sonar but does however present an oversimplified picture of the returning wavefronts. Fig.3 gives an exaggerated, but otherwise more realistic, picture of what a complete wavefront from just one region of the sea bed might look like. It will be appreciated from Fig.3 that the declination angle and depth deduced from measurements of wavefront angle can be in error. It is of interest to know by how much.

<u>A Model for Calculating Backscattered Wavefronts</u>

At any instant in time the region of the sea bed which contributes to the backscattered signal is small (Fig.1). It can be thought of containing a large number of sources which interfere to cause a wavefront such as that in Fig.3. With a particular set of such sources it is possible to compute the wavefront shape. If however our interest in the wavefront shape is confined to the vertical plane it is sufficient to consider a one dimensional array of sources (Fig. 4). For a particular set of such sources it is easy to compute the amplitude and phase at a receiver position P. If we have an odd number, $2N+1$, of equally spaced sources, distance b apart, and their amplitudes are given by

$a_{-N}, a_{-N+1}, \ldots a_0, \ldots a_{N-1}, a_N$ and their phases by

$\alpha_{-N}, \alpha_{-N+1}, \ldots \alpha_0, \ldots \alpha_{N-1}, \alpha_N$, the resultant signal at a point P which is distance R from the centre sources is given by

$$s(t,\gamma) = \sum_{n=-N}^{N} a_n e^{j\left(\omega t + \frac{2\pi R}{\lambda} + \alpha_n + \frac{2\pi n b}{\lambda}\sin\gamma\right)}$$

where γ is defined by Fig.4. This formula is valid as long as the range R is greater than the Fresnel distance corresponding to the length L of the scattering region ($L = 2Nb$). A slightly more complex equation must be used if the point P is inside the Fresnel distance but the computations are still very straightforward.

If the length L were infinitely small the computations would give the same phase for the resultant signal at all points on the circle of radius R, whatever the angle γ. For realistic values of L the phase shows significant variations with γ and some results have been obtained for the following parameters which are appropriate to the bathymetric sidescan sonar.

$\lambda = 0.366$ cm
range = 36.6m = 10,000 wavelengths
$\gamma = 20°$ to $70°$ (= declination angle θ for a flat sea bed)
pulse length = 160 μs, corresponding to a range resolution of 12cm

The mid-value of γ in the computation is 45° and, based upon this, the sources are considered to be distributed over a distance of $\sqrt{2}$ times the range resolution (Fig.5). The computer model uses 47 sources at a spacing of one wavelength, or 0.37cm. It is thought appropriate that the sources should have a random phase and a Rayleigh distribution of backscattering amplitude. This is achieved in the model by giving each source a pair of quadrature amplitude components taken from a table of random normal numbers of zero mean and unity standard deviation. The amplitude and phase of the resultant waveform has been calculated along the circumference of a circle whose radius is 10,000 wavelengths. Care is taken to follow any excursions in the phase outside the range of $\pm\pi$. The radial deviations of zero phase points from the circle are then calculated by dividing the computed phase by 2π. This is valid so long as the far field approximation of Eq.1 is valid because then the range dependent term affects each component term equally.

It is desirable to exaggerate the wavefront crinkles on a display in order to render them more apparent and Fig.6 adopts polar coordinates in which the horizontal scale is very much greater than that of the vertical scale.

The Lateral Displacement of the Scattering Region

It can be argued as follows that the apparent lateral displacement of the scattering region in metres is independent of range. Considering Eq.1 it can be seen that there is only one term involving range and this can be taken outside the summation. If we have two receivers at the same range R, one at angle γ and the other at angle $\gamma + \Delta\gamma$, it follows that the phase difference does not depend on the value of R but only on the value of γ and the angular separation of the receivers $\Delta\gamma$. If $\Delta\gamma$ is very small such that the wavefront is linear between the two receivers it must follow that, at a particular value of γ, the phase difference ϕ_D is proportional to $\Delta\gamma$

$$\phi_D = k\Delta\gamma$$

But $\Delta\gamma = d/R$ where d is the linear separation of the two receivers

$$\therefore \quad \phi_D = k\frac{d}{R}$$

i.e. At a particular angle, ϕ_D is inversely proportional to range for a constant linear separation of the two receivers.

Consider the scattering region to be on the boresight of the two receivers. The apparent lateral displacement of the scattering region is $R\theta'$ where θ' is the deviation of the incident wavefront and is related to the phase difference measurement by $\theta' = \sin^{-1}(\lambda\phi_D/2\pi d) = \lambda\phi_D/2\pi d$ if θ' is small. It follows that the lateral displacement $R\theta'$ is given by

$$R\theta' = R\frac{\lambda}{2\pi d}\cdot\frac{kd}{R} = \frac{k\lambda}{2\pi}$$

i.e. the apparent lateral displacement of the scattering region in metres is range independent. This suggests the very informative display of the scattering region displacement shown in Fig.8. This result is valid whatever the range. An alternative terminology for the displacement is 'glint'.

The glint shown in Fig.8 is a sideways displacement. The corresponding depth error of the bathymetric sidescan sonar is slightly less because of a geometric factor ($\sqrt{2}$ when at a declination angle of 45° as indicated in Fig.7)

Probability of Error

Fig.8 is a plot of glint as a function of angle for typical system parameters and gives a very clear picture of how depth measurements can be in error.

By calculating the glint at very many angles and performing a statistical analysis it would be possible to derive a probability density function or a cumulative distribution function of the glint. However it is more elegant to make use of an analytical expression for the p.d.f. of the phase difference $p(\phi_D)$ which is available from the results of Cooper and Wyndham(6). Their equation for $p(\phi_D)$ and a simplified version applicable to the sea bed profiling sonar situation are presented in the Appendix.

Using the simplified formula $p(\phi_D)$ is plotted in Fig.9 for the case where $d\Delta\theta/\lambda = 0.036$ which might correspond, for example, to a receiver separation of three wavelengths, a pulse length of 160 µs (which is equivalent to a range resolution of 12 cm), and a range of 10 m, and a declination angle of 45°. In Fig.10 $p(\phi_D)$ is plotted for the case where $d\Delta\theta/\lambda = 0.0036$ which might correspond, for example, to a receiver separation of three wavelengths, a pulse length of 160 µs, a range of 100 m and a declination angle of 45°. In both of these cases the depth error is related to ϕ_D by the formula

$$\text{depth error} = \sin\theta \cdot R\,\theta' = \frac{R}{\sqrt{2}} \sin^{-1} \frac{\lambda\phi_D}{2\pi d}$$

Considering Fig.10, the rapidly decaying tails might suggest that phase difference errors of more than, say, 0.025 radians are negligible. In fact however the tails decay much less rapidly than those, say, of a Gaussian function and it is very informative to plot the probability of a particular value of ϕ_D being exceeded. Table 1 presents some results calculated numerically from the p.d.f. of Fig 10.

Table 1

ϕ (radians)	0	0.0125	0.025	0.05	0.1	0.2
Prob($\lvert\phi_D\rvert > \phi$)	100%	11.4%	3.17%	0.8%	0.2%	0.05%

The probability of the phase difference being in error by more than 0.1 radian is 0.2%. Considering $d/\lambda = 3$ and $r = 100$m this is equivalent to saying that there is 0.2% probability that the depth measurement error exceeds 0.4m. In practical terms this fortunately indicates a very adequate system performance. Furthermore it is easy to prove and interesting to note that, for a constant pulse length, the depth inaccuracy is to a good approximation independent of range and of transducer spacing (the wavefront angle is what counts, not the phase difference). The pulse length is however very important and, as an example, an increase in pulse length by a factor of three to 480 µs can be shown to cause the depth error which is exceeded with 0.2% probability to rise by a factor of three to 1.2m.

Depth errors based on such low probabilities as 0.2% might be seen to be insignificant. However it should be appreciated that a short spike on a depth profile might be interpreted as some important sea bed feature. Furthermore there are a large number of independent range resolution cells contained within the operating range of the sonar and events with the low probability of 0.2% can still occur several times per transmission.

A major reduction in inaccuracy occurs if depth measurements from neighbouring resolution cells are averaged. In the cross-track direction this can be achieved electronically using a filter; in the along-track direction it can be achieved by trace-to-trace integration.

Glint and its effect on the Accuracy of a Sea Bed Profiling Sonar

Conclusion

A model has been used in which the scattering region is assumed to contain a large number of independent sources with Rayleigh distributed amplitudes and uniformly distributed phases. There is little doubt that certain configurations of sources could give greater wavefront irregularities and that an actual region of the sea bed might well fall in such a category. However the general conclusions are still the same. It has been shown that a good depth accuracy goes hand in hand with good range resolution. The pulse length should be kept short in a sea bed profiling sonar for a high accuracy of depth measurement. A suitable design criterion is to make the pulse length in water about five times less than the required depth accuracy.

References

1. Cram,L.A.: "Modelling Methods of Determining Radar Echo Characteristics" Agard Lecture Series No.59, Paper 1(e)
2. Woolcock,S.C.: "Target Characteristics" Agard Lecture Series No.59 Paper 2(a)
3. Denbigh,P.N.: "A Bathymetric Sidescan Sonar", Ultrasonics International 79, pp 321 - 326
4. Denbigh,P.N.: "Stereoscopic Sidescan Sonar", Acoustics Letters, Vol.7, (1979), pp 108-112.
5. Denbigh,P.N.,and Weighton,D.M.: "The Design of Sidescan Arrays and the Elimination of Vertical Sidelobes", Institute of Acoustics Specialist Meeting on Transducer Arrays and Array Processing (1978), pp 11 - 18.
6. Cooper,D.C.,and Wyndham,B.A.: "A Comparison of Monopulse Techniques for Direction Finding in the Presence of Interference", Radar - present and future, IEE Conf.Publ.105, 1973, pp 154 - 159.

APPENDIX

The analysis of Cooper and Wyndham is more extensive than needed here because they examine direction finding techniques which compare the relative amplitudes from receivers with overlapping beams as well as direction finding techniques which measure phase difference. Furthermore their analysis includes situations in which an unwanted signal is present as well as the wanted signal. It is assumed that both wanted and unwanted signals arise from scatterers with Rayleigh distributed amplitudes and uniformly distributed phases. The probability density function for the phase difference is given by

$$p(\phi_D) = \frac{D^2}{2\pi\sigma_1^2\sigma_2^2}\left[\frac{1}{1-\Phi_1^2} - \frac{\Phi_1}{(1-\Phi_1^2)^{3/2}}\left\{\frac{\pi}{2} - \sin^{-1}\Phi_1\right\}\right]$$

where $$\Phi_1 = \frac{\eta\sin\phi_D - \rho\cos\phi_D}{\sigma_1\sigma_2} \quad , \quad D = \sigma_1^2\sigma_2^2 - \rho^2 - \eta^2$$

and
$$\sigma_i^2 = \int_0^{2\pi} \{S(\theta)+I(\theta)\}\{B_i(\theta)\}^2 d\theta \qquad i=1,2$$

$$\rho = \int_0^{2\pi} \{S(\theta)+I(\theta)\} B_1(\theta) B_2(\theta) \cos\{\beta_2(\theta)-\beta_1(\theta)\} d\theta$$

$$\eta = \int_0^{2\pi} \{S(\theta)+I(\theta)\} B_1(\theta) B_2(\theta) \sin\{\beta_2(\theta)-\beta_1(\theta)\} d\theta$$

where $S(\Theta)$ = signal power density
$I(\Theta)$ = interference power density (assumed zero in our case)
$B_i(\Theta)$ = amplitude response of channel i
$\beta_i(\Theta)$ = phase response of channel i

Considering the amplitude responses to be isotropic

$$\{B_1(\Theta)\}^2 = \{B_2(\Theta)\}^2 = \frac{1}{2\pi}$$

If the scattering region subtends an angle $\Delta\Theta$ about the receivers

$$S_1(\theta) = S_2(\theta) = \frac{2\pi}{\Delta\theta} \qquad \text{over } \Delta\theta$$

$$\therefore \quad \sigma_1^2 = \sigma_2^2 = \int_{-\Delta\theta/2}^{\Delta\theta/2} \frac{1}{\Delta\theta}\, d\theta = 1$$

$\{\beta_2(\Theta) - \beta_1(\Theta)\}$ is the phase difference between the two channels for a wave arriving from angle Θ and is given by

$$\beta_2(\theta) - \beta_1(\theta) = \frac{2\pi d \sin\theta}{\lambda}$$

where d is the receiver separation.

The formula for the p.d.f. can be used for a signal arriving at any required angle Θ relative to the boresight of the two receivers. However the results do not vary greatly over a typical operating sector of up to $\pm 30°$ and it is helpful to consider a signal centred on the boresight because $\sin\{\beta_2(\Theta) - \beta_1(\Theta)\}$ then has odd symmetry reducing η to zero and ρ to sinc $(\pi d\Delta\Theta/\lambda)$.

Thus the formula for $p(\phi_D)$ can be simplified to

$$p(\phi_D) = \frac{1-\rho_B^2}{2\pi(1-\rho_B^2\cos^2\phi_D)}\left[1 + \frac{\rho_B\cos\phi_D\{\frac{\pi}{2}+\sin^{-1}(\rho_B\cos\phi_D)\}}{(1-\rho_B^2\cos^2\phi_D)^{1/2}}\right]$$

where ρ_B signifies the value of ρ on the boresight and equals $\mathrm{sinc}(\pi d\Delta\Theta/\lambda)$.

Glint and its effect on the Accuracy of a Sea Bed Profiling Sonar

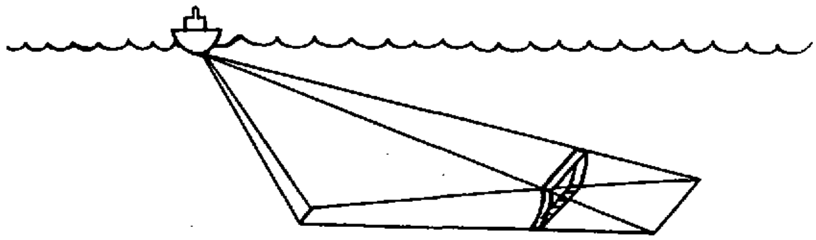

Fig.1 Side-scan sonar geometry

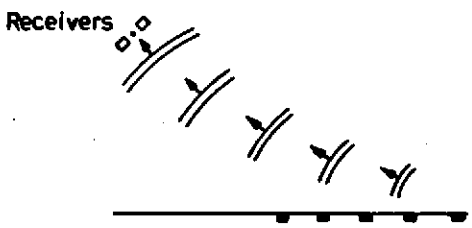

Fig.2 Backscattered wavelets

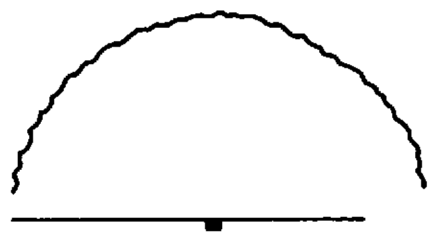

Fig.3 Wavefront fine structure

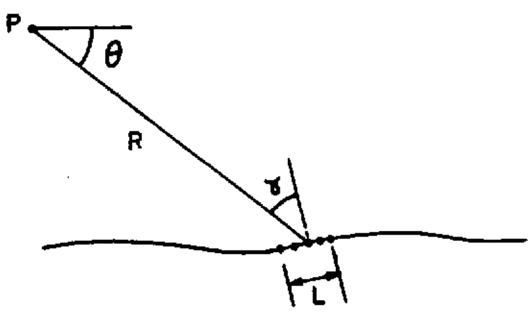

Fig.4 Model of scattering sources

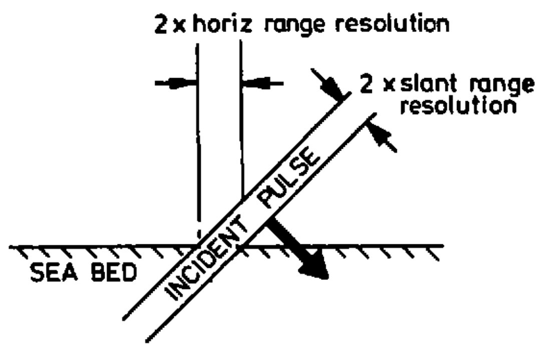

Fig.5 Range resolution of sonar

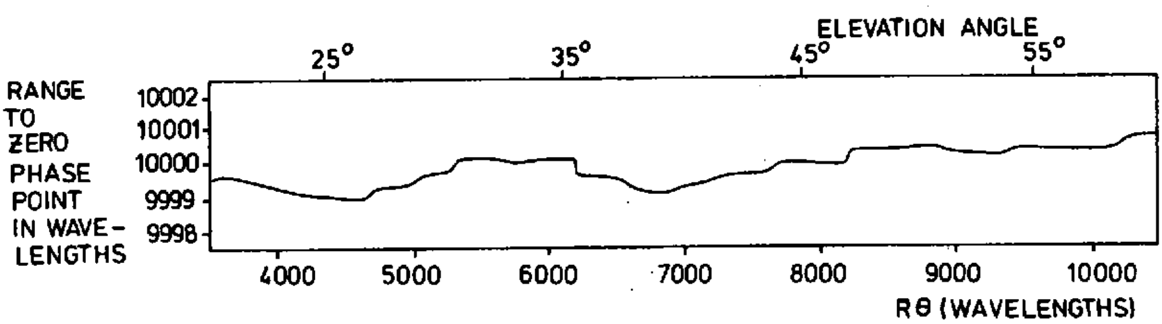

Fig.6 Computed wavefront shape

Glint and its effect on the Accuracy of a Sea Bed Profiling Sonar

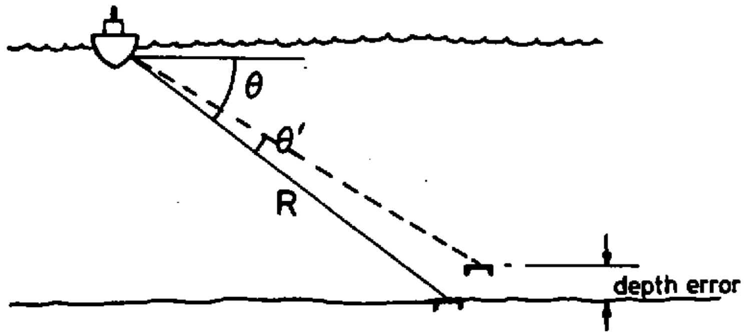

Fig.7 The effect of angular error on depth error

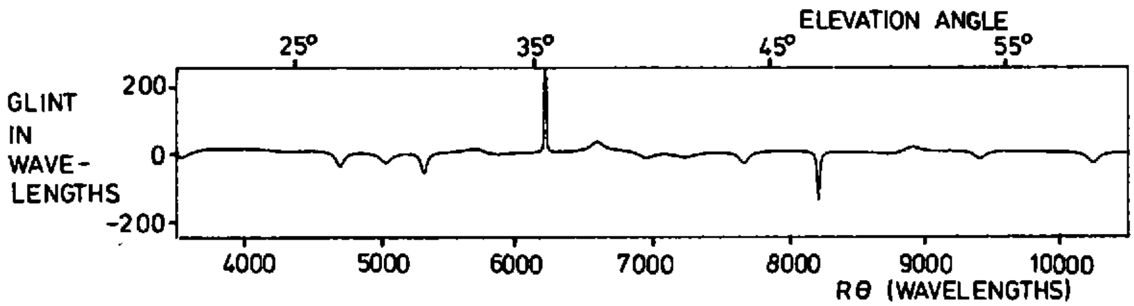

Fig.8 Computed glint as a function of sonar position relative to a particular scattering region on the sea bed.

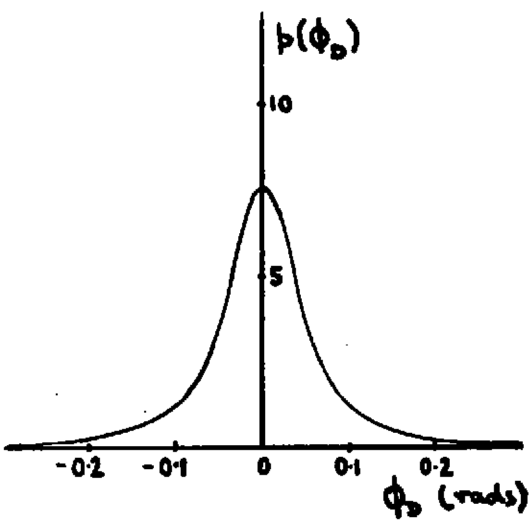

Fig.9 p.d.f. of phase difference when $d\Delta\theta/\lambda = 0.036$

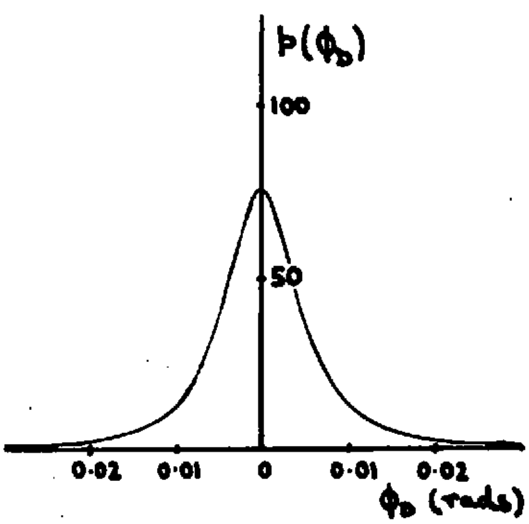

Fig.10 p.d.f. of phase difference when $d\Delta\theta/\lambda = 0.0036$